

BRAIN COMMUNICATIONS

Right fronto-parietal networks mediate the neurocognitive benefits of enriched environments

Méadhbh B. Brosnan,^{1,2,3,4}  Nir Shalev,^{1,2,3} Jivesh Ramduny,^{5,6,7}
 Stamatios N. Sotiropoulos^{7,8} and  Magdalena Chechlac^{9,10}

Exposure to enriched environments throughout a lifetime, providing so-called reserve, protects against cognitive decline in later years. It has been hypothesized that high levels of alertness necessitated by enriched environments might strengthen the right fronto-parietal networks to facilitate this neurocognitive resilience. We have previously shown that enriched environments offset age-related deficits in selective attention by preserving grey matter within right fronto-parietal regions. Here, using neurite orientation dispersion and density imaging, we examined the relationship between enriched environments, microstructural properties of fronto-parietal white matter association pathways (three branches of the superior longitudinal fasciculus), structural brain health (atrophy), and attention (alertness, orienting and executive control) in a group of older adults. We show that exposure to enriched environments is associated with a lower orientation dispersion index within the right superior longitudinal fasciculus 1 which in turn mediates the relationship between enriched environments and alertness, as well as grey and white matter atrophy. This suggests that enriched environments may induce white matter plasticity (and prevent age-related dispersion of axons) within the right fronto-parietal networks to facilitate the preservation of neurocognitive health in later years.

- 1 Department of Experimental Psychology, University of Oxford, Oxford, UK
- 2 Oxford Centre for Human Brain Activity, University of Oxford, Oxford, UK
- 3 Wellcome Centre for Integrative Neuroimaging, University of Oxford, Oxford, UK
- 4 Turner Institute for Brain and Mental Health, Monash University, Melbourne, VIC, Australia
- 5 School of Psychology, Trinity College Dublin, Dublin, Ireland
- 6 Trinity College Institute of Neuroscience, Trinity College Dublin, Dublin, Ireland
- 7 Sir Peter Mansfield Imaging Centre, School of Medicine, University of Nottingham, Nottingham, UK
- 8 National Institute for Health Research (NIHR), Nottingham Biomedical Research Centre, Queen's Medical Centre, Nottingham, UK
- 9 Centre for Human Brain Health, University of Birmingham, Birmingham, UK
- 10 School of Psychology, University of Birmingham, Birmingham, UK

Correspondence to: Magdalena Chechlac
Centre for Human Brain Health
University of Birmingham
Birmingham B15 2TT, UK
E-mail: m.chechlac.1@bham.ac.uk

Correspondence may also be addressed to: Méadhbh B. Brosnan
Department of Experimental Psychology
University of Oxford
Oxford OX2 6GG, UK
E-mail: meadhbh.brosnan@psy.ox.ac.uk

Keywords: cognitive ageing; reserve; brain resilience; superior longitudinal fasciculus; diffusion MRI

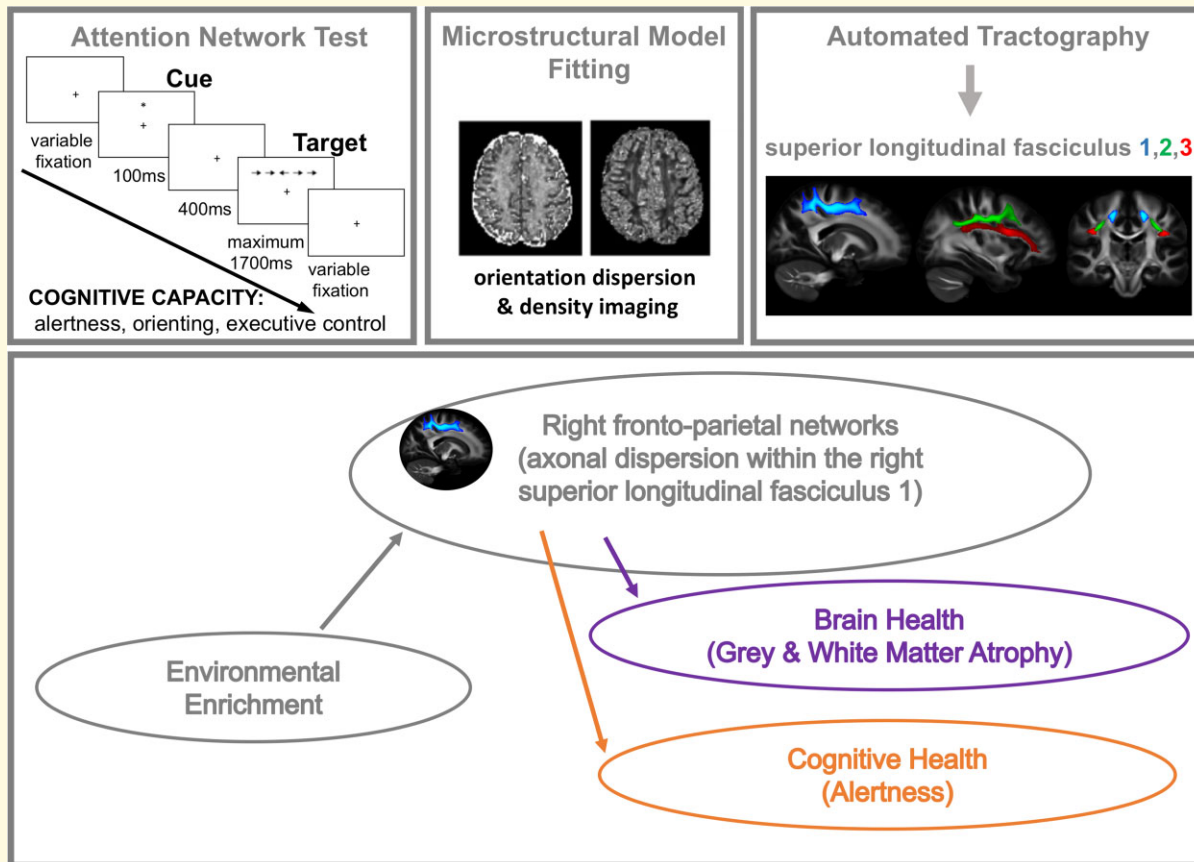
Received September 06, 2021. Revised January 10, 2022. Accepted March 25, 2022. Advance access publication March 28, 2022

© The Author(s) 2022. Published by Oxford University Press on behalf of the Guarantors of Brain.

This is an Open Access article distributed under the terms of the Creative Commons Attribution License (<https://creativecommons.org/licenses/by/4.0/>), which permits unrestricted reuse, distribution, and reproduction in any medium, provided the original work is properly cited.

Abbreviations: ANT = Attention Network Test; CRI = Cognitive Reserve Index; CRIq = Cognitive Reserve Index questionnaire; dMRI = diffusion MRI; DTI = diffusion tensor imaging; EE = enriched environment; FA = fractional anisotropy; FP = first fixation period; FPN = fronto-parietal network; GM = grey matter; GMVa = grey matter volume atrophy; ICVF = intra-cellular volume fraction; LC-NE = locus coeruleus norepinephrine; NODDI = neurite orientation dispersion and density imaging; ODI = orientation dispersion index; rSLF = right superior longitudinal fasciculus; RT = reaction time; SLF = superior longitudinal fasciculus; WM = white matter; WMVa = white matter volume atrophy

Graphical Abstract



Introduction

In the foreword to the 2020 World Health Organization (WHO) landmark report on healthy ageing, Dr Tedros Adhanom Ghebreyesus (WHO Director-General) states that ‘Humans now live longer than at any time in history. But adding more years to life can be a mixed blessing if it is not accompanied by adding more life to years’. An integral component of living life to the fullest in our later years is the capacity to maintain adequate cognitive abilities in older age. But human ageing is characterized by a sheer diversity of trajectories, with some older adults maintaining almost youth-like physical and cognitive capacities, and others experiencing frailty, disability and dementia. Multiple modifiable factors across a lifetime have been shown to influence the trajectories of cognitive ageing.¹ Older adults who have engaged in cognitively and socially enriched environments (EEs) exhibit greater resilience to cognitive decline when

faced with neuropathological conditions such as Alzheimer’s disease,^{2–5} a phenomenon referred to as neurocognitive reserve, cognitive reserve or simply reserve.^{4,6–8} The concept of reserve originates from long-standing observations with Alzheimer’s patients whereby higher levels of education attainment delay the onset time of clinical symptoms of the disease and, consequently, cognitive decline.^{2,4,9} However, it is increasingly evident that such benefits to neurocognitive health are not exclusively obtained through education, but are additionally noted for leisure and social activities, and occupational engagements throughout a lifetime.^{10,11} Correspondingly, it has been proposed that a variety of enriched and engaging environments across a lifetime contribute to optimal brain health and to prevent, or at least delay, the onset of dementia later in life.^{4,12} Yet despite compelling, large-scale longitudinal evidence for this phenomenon, we are just beginning to understand the

neurobiological basis by which EEs impact the brain to cultivate resilience.

EEs necessitate the continued engagement of several core cognitive processes, including alertness, sustained attention and awareness, all of which rely on the right fronto-parietal networks.^{13–20} Continued activation of these right lateralized networks has been theorized to cultivate and support the neuroprotective phenomenon of cognitive reserve.²⁰ The locus coeruleus norepinephrine (LC-NE) alertness system has strong projections to the right fronto-parietal networks,^{21–27} and the strengthening of these networks by EEs over a lifetime is proposed to arise from the continued engagement of the LC-NE system over extended periods.²⁰

Numerous studies provide evidence that cognitive experiences (e.g. training or learning new skills) result in experience-dependent brain changes in brain structure in both the grey and white matter (WM) regions (i.e. structural plasticity changes).^{28–30} As such, the beneficial influence of a lifelong exposure to EE on cognitive performance later in life may be understood in terms of structural plasticity processes which may optimize brain functioning and cognitive performance^{31,32} to offset neuroanatomical deficits relating to poor brain health (e.g. structural atrophy).³³

Our previous work using mathematical models of visual attention,³⁴ causal manipulation techniques^{34,35} and voxel-based morphometry³⁶ provide increasing support for the proposal that EE may facilitate neuroprotective resilience through specifically impacting the structural [grey matter (GM) volume] and function (lateralized asymmetry of visual processing speed) of right hemisphere fronto-parietal regions (see Van Loenhoud *et al.*³⁷ and Robertson *et al.*^{19,20} for a detailed review theorizing right lateralized underpinnings of reserve). Cortical regions within the fronto-parietal networks are connected by WM association pathways comprising three branches of the superior longitudinal fasciculus (SLF) (SLF1, SLF2 and SLF3).³⁸ Our recent work suggests that EE offsets age-related deficits in selective attention by preserving GM within right fronto-parietal regions.³⁶ Here we test whether the WM microstructure of the right SLF might be cultivated by EE to facilitate better maintenance of attention function in older adults.

WM pathways underpin the efficiency of communication between discrete cortical regions. Physical characteristics, including micro- and macrostructural properties of the WM (including volume, axonal diameter, myelination, fibre coherence and neurite density) influence both the neurophysiological function of the tract and functional connectivity, with subsequent consequences for behaviour.^{39–42} For example, in younger adults, inter-individual differences in the ability to efficiently attend and respond to sensory information vary according to the WM organization of the SLF.^{40,42,43} WM changes associated with the ageing process affect connectivity within neural networks and underlie gradual age-related declines in cognition.^{44–47} In contrast to invasive animal studies and post-mortem anatomical and histological human studies, microstructural properties of WM and age-related WM changes can be non-invasively studied in the living human brain with diffusion MRI (for recent review, see Lerch *et al.*⁴⁸). While

diffusion MRI only provides indirect estimates of biological properties of the WM, new developments in acquisition and data modelling increasingly enable more robust and biologically plausible measures of WM microstructural properties.^{48–51} Diffusion tensor imaging (DTI) based on conventional single-shell acquisition protocols and DTI-derived microstructural measures of WM properties, such as fractional anisotropy (FA) and mean diffusivity, have been widely employed to study age-related WM changes.^{45–47,52} However, while DTI-derived measures are indeed sensitive to age-related alterations in WM microstructure, these are non-specific measures, which cannot be attributed to specific changes in tissue microstructure.^{53,54} For example, age-related reduction in FA might be a result of decreased neurite density, changes in fibre orientation dispersion and/or other changes such as in the degree of myelination.^{50,54} In contrast, multi-shell acquisition protocols combined with biophysically plausible models have been shown to provide more specific estimates of the microstructural properties of WM tissue.⁴⁸ One such approach is neurite orientation dispersion and density imaging (NODDI),⁵⁰ which has been previously used to provide detailed accounts of WM changes associated with development, ageing and several neurological disorders.^{55–63} NODDI-derived parameters, intra-cellular volume fraction (ICVF) and the orientation dispersion index (ODI), respectively, measure neurite packing density and dispersion of neurites/axons (an estimate of fibre coherence).⁵⁰ These two parameters are effectively independent features encoded in the FA, both providing a more biologically specific model of observed changes, which could not previously be disentangled from FA measures derived from DTI. For example, previous research suggests that an increase in FA during development is driven by increasing neurite density, while a reduction in FA later in life is driven by the increase in ODI.⁵⁸ Moreover, changes in NODDI-derived parameters have been shown to be more sensitive to ageing and predictive of cognitive performance.^{55,64}

In the present study, we use NODDI to examine the relationship between microstructural properties of the SLF, EEs (measured by proxies such as education, professional, leisure and social activities), attentional capacity (representing cognitive processes contributing to reserve) and structural brain health (GM and WM atrophy) in a group of older adults. To assess attention function, we used a well-established task (the Attention Network Test; ANT).^{65–67} The ANT has been developed to measure three partially distinct ‘networks’ supporting attention: *alerting* attention in response to a temporally predictive cue, *orienting* attention in space and exerting *executive control* to resolve conflict and enhance relevant information. To corroborate the proposal that cognitively stimulating environments and experiences across the lifetime strengthen the right lateralized fronto-parietal networks to facilitate neurocognitive health later in life, we hypothesize that EE induces WM plasticity (prevents age-related dispersion of neurites and/or reduction in neurite density) within the right SLF to facilitate better maintenance of attention function (specifically alertness) and superior brain health (less volume atrophy) in older adults.

conditions (see Fig. 1). These are as follows: a central cue, where a central warning signal (an asterisk) is presented; a double cue, where two asterisks are presented indicating the two possible locations of the flanked target along the horizontal line; a spatial cue indicating where the target will appear using a single asterisk; and no cue. The cue is always presented for 100 ms and followed by another fixation period of 400 ms. A fixation cross remains at the centre of the screen throughout the trial, with the exception of the central-cue condition where it is replaced for 100 ms by an asterisk. The target surrounded by flankers is always presented either until the participant responds to reaction time (RT) or in the case of no response for a maximum of 1700 ms. In total, each trial lasts for 4000 ms (Fig. 1). Thus, once the target and flankers disappear, the next trial is preceded by a variable fixation interval based on the duration of FP and RT.

ANT task procedure

Participants were instructed to attend to the central fixation cross and to use the mouse buttons to indicate the direction of the flanked arrow when presented (i.e. left mouse click for leftward arrowheads and right mouse click for rightward arrowheads). The various conditions (four different cues and three levels of congruency) were randomized within blocks. The task began with 24 practice trials with feedback, followed by three blocks without feedback. Within each block, there were 96 trials, presented in random order. These consisted of cue condition (x4), target locations (x2), target directions (x2), flanker conditions (x3), repetitions (x2). The practise block took ~2 min, and each subsequent experimental block took ~5 min to complete.

Measuring attentional capacity (ANT scores)

We derived the ANT scores (alertness, orienting and executive control/conflict) as per previously published work^{65,74} by calculating the difference between the mean RT of the different conditions (defined by either cue or target type in the ANT procedure). The alertness score was calculated by subtracting the mean RT in the double-cue condition (i.e. the two warning cues corresponding to the two possible target locations) from the mean RT in the no-cue condition (alerting = $RT_{no\ cue} - RT_{double\ cue}$). As such, the alerting score indicates the degree to which an individual uses the external cues to benefit their reaction times. Larger alerting scores indicate a relative difficulty in maintaining alertness in the absence of an external cue i.e. decreased ability to rely on internal (or intrinsic) alertness.⁷⁴ However, it is possible that larger alertness scores might instead indicate a more efficient use of the cue. One way to dissociate the two is by testing for a correlation between the *alerting* score and the mean reaction time from the no-cue condition. A positive association would imply that participants who relied more on the alerting cue to facilitate performance were slower, thereby indicative of decreased intrinsic alertness capacities. The orienting is calculated by subtracting the mean RT in the spatial-cue condition from the mean RT in the central-cue condition (orienting = $RT_{central\ cue} - RT_{spatial\ cue}$). The spatial cue, which is always

valid, provides information about subsequent target location and thus facilitates orienting attention before target arrival. As such, the orienting score reflects the difference between responses to targets that follow spatially predictive and non-predictive cues. Larger orienting scores indicate a better capacity to orient attention and select sensory input.⁶⁵ Finally, the executive control score is calculated by subtracting the mean RT in the congruent condition from the mean RT in the incongruent condition across all cue types (executive control/conflict = $RT_{incongruent} - RT_{congruent}$). The conflict score represents the capacity to resolve response conflict to targets that appear among distractors. The larger conflict score indicates less ability (difficulty) in resolving conflict.⁷⁴ We present descriptive statistics and estimate the Pearson correlations among the four task indices: alerting, orienting, conflict and mean reaction time (RT).

Fronto-parietal microstructure

MRI data acquisition

T_1 -weighted scans (MPRAGE with spatial resolution $1 \times 1 \times 1\text{ mm}^3$) and multi-shell diffusion-weighted images were acquired at the Birmingham University Imaging Centre using a Philips 3T Achieva MRI system with a 32-channel head coil. The multi-shell diffusion acquisition comprised a single-shot EPI, $2 \times 2 \times 2\text{ mm}^3$, $5 \times b = 0\text{ s/mm}^2$, $50 \times b = 1000\text{ s/mm}^2$, $50 \times b = 2000\text{ s/mm}^2$ plus $5 \times b = 0\text{ s/mm}^2$ phase encoding-reversed to correct for susceptibility-induced artefacts.⁷⁵ T_1 -weighted scans were acquired with the following parameters: 176 slices, TR = 7.5 ms, TE = 3.5 ms and flip angle = 8° . Diffusion-weighted scans were acquired with the following parameters: 56 slices, TR = 9000 ms, TE = 81.5 ms and flip angle = 90° . All scans were visually inspected during and after the acquisition to ensure that there have not been any artefacts associated with excessive head movement and signal dropouts. All data passed this quality assessment.

T_1 -weighted data pre-processing and total grey matter volume estimation

T_1 -weighted scans were pre-processed using the UK Biobank T_1 -weighted pipeline,⁷⁶ which was used to correct for bias fields, apply skull-stripping and align data to the MNI152 standard space [a non-linear registration to MNI152 using FMRIB's non-linear image Registration Tool (FNIRT), was applied^{77,78}], before segmenting the T_1 images into different tissue classes, i.e. GM, WM and CSF using FMRIB's Automated Segmentation Tool⁷⁹. These data were subsequently used to calculate total GM and total WM volume in mm^3 , normalized for head size using SIENAX package.⁸⁰

Diffusion data pre-processing, microstructural model fitting and SLF tractography

Diffusion-weighted scans were pre-processed using the UK biobank pipeline⁷⁶ (Fig. 2). The diffusion-weighted pre-processing was applied to correct for susceptibility-induced

distortion, eddy-current distortion and participant movement induced distortions using the EDDY toolbox⁸¹ and to obtain transformations of the diffusion to structural and standard space. Specifically, the corrected dMRI data were linearly registered to structural space, using a rigid body transformation (FMRIB's Linear Image Registration Tool,^{82,83}). Structural data were non-linearly registered to standard space using FNIRT. Concatenating the two provided a non-linear transformation from diffusion to standard space. Subsequently, we applied the NODDI model to the multi-shell EDDY-corrected diffusion data^{50,84} using the CUDA Diffusion Modelling Toolbox (<https://users.fmrib.ox.ac.uk/~moisesf/cudimot/>)⁸⁵ to estimate voxel-wise microstructural parameters, including ICVF, and ODI. In addition, a diffusion tensor model⁸⁶ was fitted to low b -value ($b = 1000$ s/mm²) shells of the EDDY-corrected diffusion data to obtain FA maps for each participant. Next, we performed automated probabilistic tractography using predefined protocols for identifying major WM tracts in the left and right hemispheres, as described in FSL's XTRACT tool (<https://fsl.fmrib.ox.ac.uk/fsl/fslwiki/XTRACT>)^{87,88}. Prior to running XTRACT, we fitted the crossing fibre model (FSL's BEDPOSTX⁸⁹) to each subject's data to estimate up to three fibre orientations per voxel and ran non-linear transformations to the MNI152 standard space. XTRACT automatically reconstructs a set of predefined white matter pathways, including the three branches of the SLF (SLF1, 2, 3). These three tracts were reconstructed and used for the purpose of data analysis. The SLFs' tract probability density maps, normalized by the total number of valid streamlines, were thresholded at 0.1% and binarized to produce a tract mask for each tract in standard space. Finally, for each participant, we calculated a set of image-derived phenotypes, characterizing different microstructural properties of the three branches of SLF. Specifically, for each tract (left and right SLF1, 2, 3), and for each DTI (FA) and NODDI (ODI, ICVF) parameter, the weighted mean value (i.e. the mean weighted by the tract probability in each voxel) of the parameters within given tract was calculated. We checked all neuroimaging measures for outliers, which were defined as any scores greater or less than three times the inter-quartile range. Based on these criteria, two participants were excluded. Subsequently, all statistical analyses as described below were conducted with a sample of $N = 47$ after the removal of these two outliers and the participant with missing CRIq data.

Statistical analyses

To assess whether environmental enrichment was differentially associated with the hemisphere-specific microstructural organization of the SLF, we modelled EE (the composite CRIq score) as a function of three separate microstructural estimates: ODI, ICVF and FA within the three SLF branches in each hemisphere using the following linear regression approach. For each model, age was entered as a nuisance covariate in the first step, and then the ODI estimates of the six

SLF branches (i.e. branches 1–3 for both hemispheres) were entered in the model using a stepwise approach. These analyses revealed that ODI (within the right SLF1) was particularly sensitive to the impact of EE. In the analyses above, EE was estimated using the composite CRIq score. To identify whether specific types of enrichment were driving the observed effect of EE on the right SLF1, a follow-up analysis of the three subscales (education, occupational and leisure engagements) was performed.

To investigate whether ODI within the SLF was associated with the degree of GM and WM volume atrophy (GMVa and WMVa, respectively) in the older individuals' brains, we modelled total GM and total WM volume (normalized for head size), as a function of ODI within the three SLF branches in each hemisphere. Again, age was entered as a nuisance regressor in step 1 for both models, and the ODI estimates for all six SLF branches were entered into each model with a stepwise approach. These analyses identified a specific association between both GMVa and WMVa with ODI within the right SLF1. We subsequently tested whether a causal association existed between EE, ODI within the right SLF1 and brain atrophy (separately GMVa and WMVa) using bootstrapped mediation analyses. For this, bootstrapped mediation analyses (5000 samples) were performed using the PROCESS computational toolbox.^{90,91} More specifically, the plausibility of a causal model was investigated, whereby EE (predictor variable X) causally influenced white matter microstructure (ODI) of the right SLF1 (mediator variable M), to in turn exert a causal influence over GMVa and WMVa in the older adults (outcome variables Y). The confidence intervals (CIs) reported for the indirect effect are bootstrapped CIs, based on 5000 samples, and are considered significant when they do not contain zero.

Finally, to determine whether the right SLF1 showed a meaningful relationship to attentional capacity, we next modelled ODI within this tract as a function of the three ANT scores (alertness, orienting and executive control) using a stepwise regression model, again with age as a nuisance covariate in the first step of the model. As we observed an association between ODI within the right SLF1 and alertness, we subsequently tested whether a causal association existed between EE, ODI within the right SLF1 and alertness using bootstrapped mediation analysis as described above (causal mediation model EE-> rSLF1 -> alertness). To explore which aspect of EE was driving our effects, a follow-up mediation analysis with the three subscales (education, occupational and leisure engagements) of CRIq was performed.

Before the analyses as described previously, all data sets were checked to ensure no statistical assumptions were violated. The normality of residuals and heteroskedasticity were tested for all analyses by visual inspection of the residuals, and formal analysis using the Shapiro–Wilks test of normality. Statistical analyses were conducted using a combination of SPSS software version 27 (IBM SPSS Statistics, NY, USA) and MATLAB r2021a (The MathWorks, Natick, MA, USA).

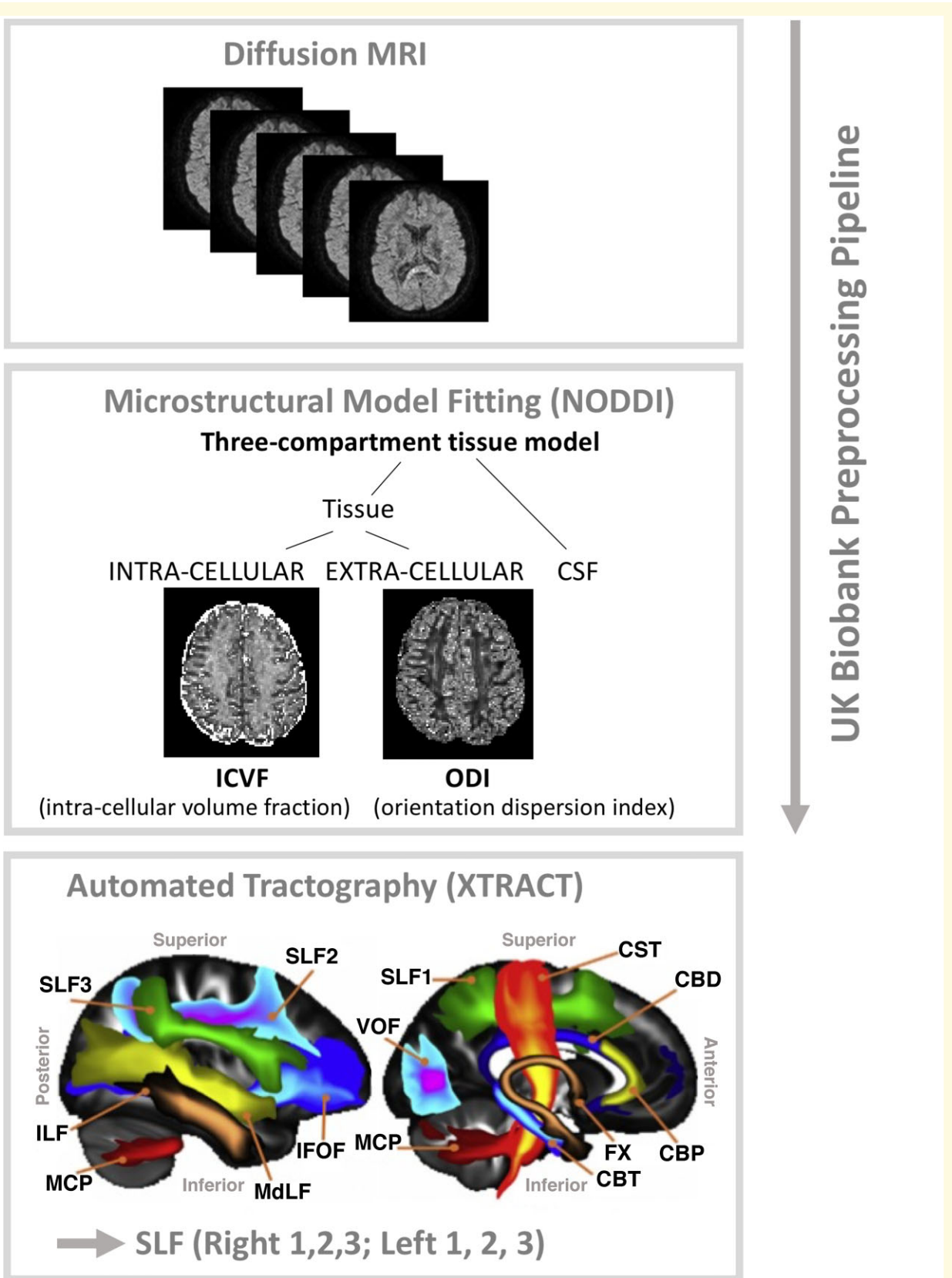


Figure 2 Overview of the diffusion MRI data analysis pipeline.

With null hypothesis significance testing, non-significant effects should not be interpreted as support for the null hypothesis.⁹² To address whether non-significant findings represented support for the null hypotheses and to verify the results from our frequentist statistics, we supplemented the above analyses using the Bayesian inference approach. For these analyses, we used JASP software (version 0.11.1, JASP Team 2019)⁹³ with the Bayesian information criterion (BIC)⁹⁴ to compare model fits. Model priors were set using the default settings in JASP (beta-binomial $a = 1$, $b = 1$). We report the $P(M|data)$ values indicating the posterior probability of each model (i.e. the probability of each model after observing the data) and consider all values >0.05 . We additionally report BF_M values which compare a given model against all other models, i.e. the factor by which the odds in favour of a given model have increased having observed the data. BF_M values above 1 indicate the strength of evidence in favour of the alternative and values below 1 indicate strength of evidence in favour of the null model.^{95,96}

Data availability statement

Participant data will be made available to researchers upon request.

Results

Attentional capacity: performance on the ANT

The overall mean accuracy was high (mean accuracy 98%; $SD = 0.02\%$; range: 9–100%) indicating that participants did not have any difficulty completing the task. Our analysis focused on RT-based indices measuring individual differences in attentional capacity, i.e. three network scores used to represent the efficiency of the alerting, orienting and executive control.^{65,74} Table 1 summarizes RT data averaged for each target and cueing condition.

The distribution of the network scores is depicted in Fig. 3A. The scattered data points illustrate that the majority of the observations were positive, thus indicating that in this cohort of older adults, most participants (i) benefitted from the alerting cue (i.e. were faster when presented with a cue); (ii) showed a good capacity to orient attention, i.e. benefitted from a spatial cue (orienting attention) before the arrival of target; and (iii) were better at judging congruent targets, compared with incongruent i.e. had decreased ability (difficulty) in resolving conflict.

As suggested in the ‘Materials and methods’ section, the interpretation of the ANT alertness measure is not straightforward as a larger alerting score could be indicative of either decreased ability to rely on internal alertness or more efficient use of a cue. We tested the correlation between the alertness score and the mean RT in the ‘no cue’ condition and found a significantly high correlation ($r = 0.56$, $P < 0.0005$; Fig. 3B). Accordingly, people who benefitted more from the alerting cue were also relatively slow when there was no cue. This is in line with the former interpretation of the alertness index such that in our sample, higher scores were associated with a lower level of internal alertness.

The mean network scores (effect), mean RT and correlations between these indices are shown in Table 2. The correlation analyses were conducted to examine independence of the attentional capacity measures. As in originally published ANT paper⁶⁵ reporting no significant correlations between network scores, we found no correlations between alerting, orienting and executive control scores indicating the independence of estimated measures of alertness, orienting and executive control. The mean RT correlated with the alerting and conflict scores.

EE mitigates neurite (axonal) dispersion in the right SLF1

We modelled EE (the composite CRIq score) as a function of ODI within the SLF branches (SLF1, 2 and 3) in each hemisphere (Fig. 4). Age was entered as the first step in the model and offered no significant improvement in model fit over the intercept only model [$R^2_{\text{change}} = 0.02$, $F_{\text{change}} = 0.94$, $P_{\text{change}} = 0.34$, unstandardized beta = 0.67, 95% CI (−0.71 2.04), $SE = 0.68$, standardized beta = 0.14, $t = 0.97$, $P = 0.34$]. Next, ODI estimates for each of the six SLF branches were entered into the model using a stepwise approach. This model offered a significant improvement in fit [$R^2_{\text{change}} = 0.12$, $F_{\text{change}} = 5.86$, $P_{\text{change}} = 0.02$, unstandardized beta = −588.41, 95% CI (−1078.12 to −98.69), $SE = 252.99$, standardized beta = −0.339, Cohen’s $F^2 = 0.16$] and led to the inclusion of the right SLF1 ($t = -2.42$, $P = 0.02$, Fig. 4), and exclusion of all other SLF branches (all $t > -1.50$, $P > 0.14$), indicating that greater EE was associated with less dispersion of neurites (lower ODI) within this tract. To obtain accurate parameter estimates of this model, not influenced by other uninformative variables, we modelled EE directly as a function of the right SLF1 and report the results in Table 3. We next assessed whether EE affects neurite density (as measured by ICVF) of the SLF using a similar modelling

Table 1 The mean RT (standard error) for each target and cueing condition

Target type	Cue type			
	No cue (ms)	Double (ms)	Central (ms)	Spatial (ms)
Neutral	717 (15.33)	665 (13.46)	693 (13.85)	637 (12.76)
Congruent	735 (16.21)	680 (12.54)	707 (15.10)	643 (13.44)
Incongruent	857 (19.02)	829 (19.48)	838 (18.05)	762 (16.90)

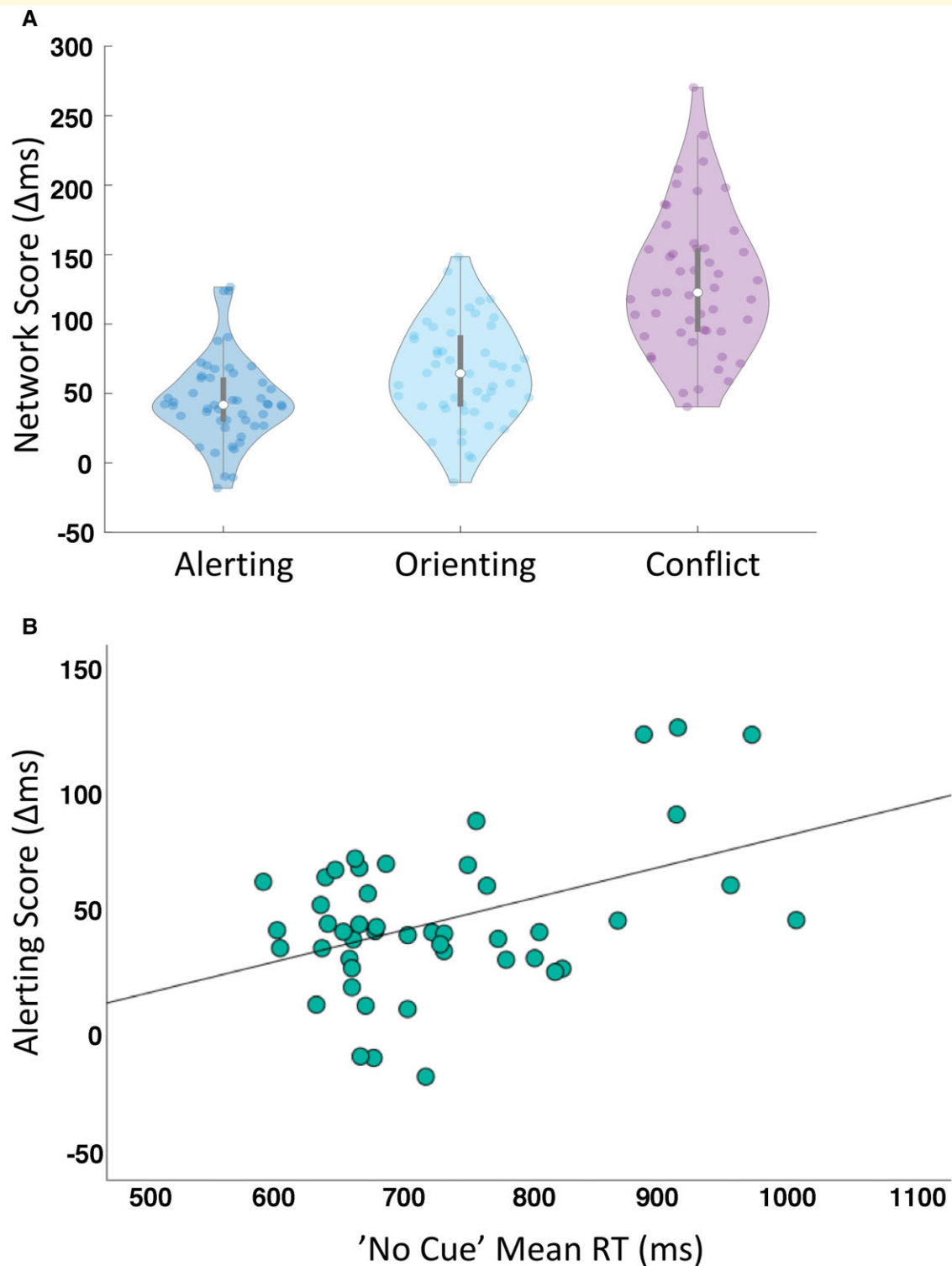


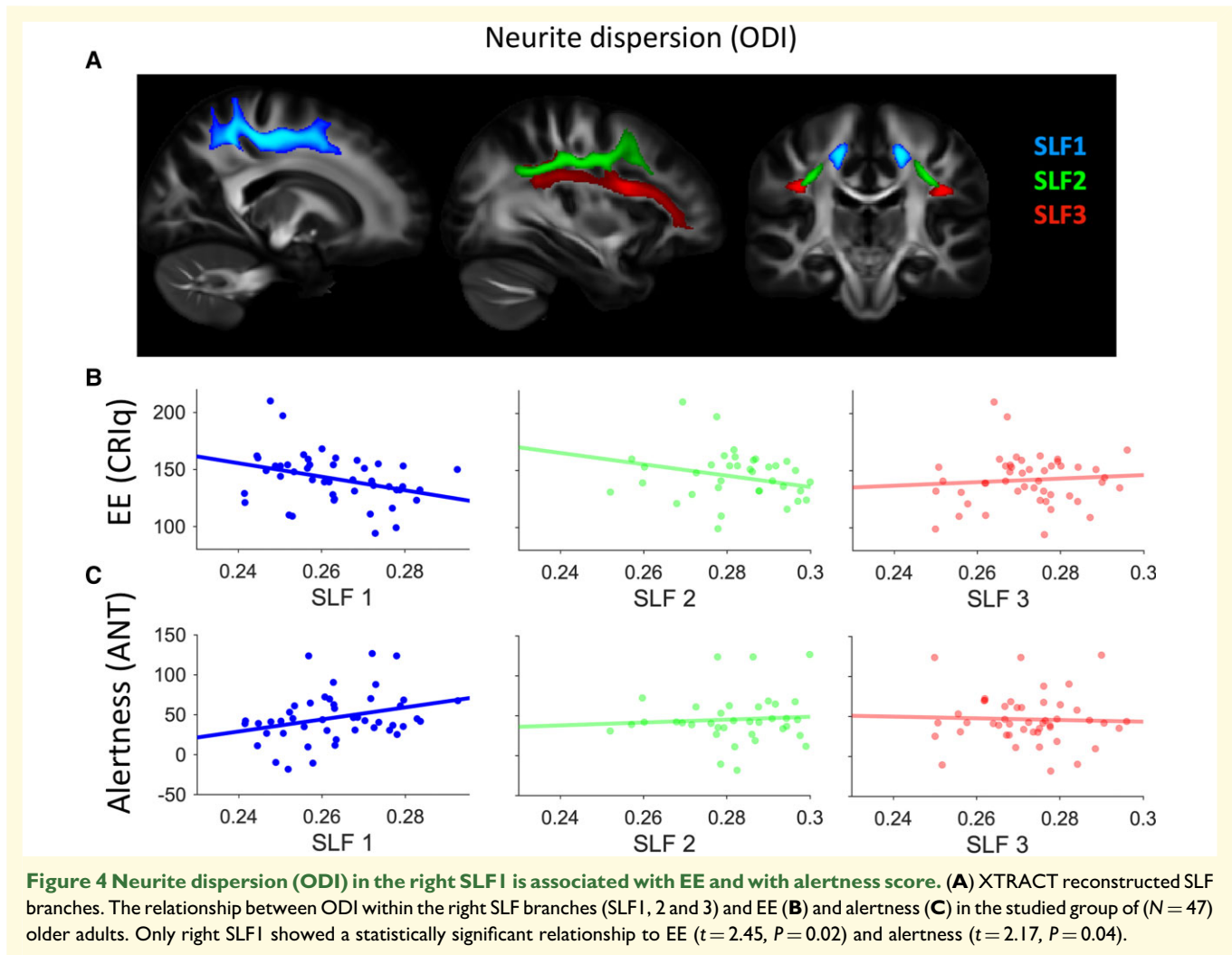
Figure 3 Performance on the ANT (derived network scores; alerting, orienting and conflict). (A) The alerting, orienting and conflict network scores based on the ANT performance are plotted to illustrate attentional capacity distribution in the studied group of ($N = 47$) older adults. (B) The scatter plot for the correlation between the alertness network score and 'no cue' mean RT ($r = 0.56$, $P < 0.0005$).

approach, this time with ICVF within the SLF branches as predictor variables. We found no evidence that EE was associated with altered neurite density (ICVF) in any of the SLF branches (all $t < 1.10$, $P > 0.28$), suggesting that EE

specifically altered neurite dispersion and not neurite density within the right SLF1. Finally, using the same modelling approach, we assessed whether EE varied as a function of FA. We found no evidence that EE was associated with

Table 2 The mean network scores (effect), mean RT (standard error) and correlations between attention networks

	ANT score	Alerting	Orienting	Conflict
Alerting (Δ ms)	45.1 (4.34)			
Orienting (Δ ms)	64.7 (5.04)	$r = 0.08$		
Conflict (Δ ms)	129.8 (7.18)	$r = 0.24$	$r = -0.12$	
Mean RT (ms)	730 (14.6)	$r = 0.39^{**}$	$r = 0.32$	$r = 0.51^{***}$

*** $p < 0.0005$.** $p < 0.005$.

altered FA within any of the SLF branches (*all* $t < 0.33$, $P > 0.13$).

To address whether the non-significant findings reported above represented support for the null hypotheses and to verify the results from our frequentist statistics, we supplemented the above analyses using the Bayesian inference approach, testing the associations between EE and white matter microstructure (ODI, ICVF and FA) of the three SLF branches in each hemisphere and age. Consistent with the frequentist statistics, the best-fitting model of EE from

the BIC analyses with ODI for all six SLF branches included ODI within the right SLF1 [$P(M|data) = 0.15$]. After observing the data, the odds of including ODI of the right SLF1 in a model of EE increased by a factor of 9.34 ($BF_M = 9.34$). The next best-fitting model contained ODI of the right SLF2 [$P(M|data) = .12$; $BF_m = 7.5$], suggesting that this right hemisphere pathway additionally varies according to EE. The $P(M|data)$ of all other models was ≤ 0.05 .

Repeating the same Bayesian model with FA of the six SLF branches indicated only one model which slightly improves

Table 3 Neurite dispersion of the right as a function of EE, GMVa, WMVa and alertness

	Unstand. β	Std error	Stand. β	T	P-value	95 % CI	Cohen's F^2
EE	-0.000198	.000081	-0.34	-2.45	0.02	(0.00036 to -0.000035)	0.13
GMVa	-1359.71	457.98	-0.41	-2.97	0.005	(-2282.13 to -437.30)	0.20
WMVa	-1416.16	578.64	-0.34	-2.45	0.02	(-2581.61 to -250.72)	0.13
ANT alerting	0.00013	0.00006	0.31	2.17	0.04	(0.000009-0.000242)	0.10

Cohen's F^2 calculated as $[R^2/(1-R^2)]$. The reported parameter estimates here are from separate models as described in the main text.

over and above the null model; FA of the right SLF2 [$P(M|data) = 0.054$]. More specifically, the odds of including FA of the right SLF2 in a model of EE increased by a factor of 3.15 after observing the data ($BF_M = 3.15$). The $P(M|data)$ of all other models were ≤ 0.03 . Finally, when modelling EE as a function of the ICVF metrics of the SLF, the $P(M|data)$ of all models was ≤ 0.025 .

The effect of EE on the right SLF1 is driven by professional engagement

Having observed that EE was associated with altered neurite/axonal dispersion within the right SLF1, we next asked the question of whether this effect was driven by any specific facet of enriching activities. Our assessment of EE (the CRIq) comprised three subscales; leisure, work and education. As such, we explored the direct association between the right SLF1 and all three subscales using a model with the right SLF1 as the dependent variable, age as a nuisance predictor in the first stage of the model and the three CRIq subscales as predictors in the second stepwise stage of the model. Age offered no significant improvement in fit [$R^2_{change} = 0.001$, $F_{change} = 0.02$, $P_{Fchange} = 0.88$, unstandardized beta = $-6.22e^5$, 95% CI (0-0), SE = 0, standardized beta = -0.02 , $t = -0.16$, $P = 88$]. However, there was a specific association between the work subscale of the CRI and the right SLF1 such that greater occupational complexity and professional engagements were associated with decreased dispersion of neurites (ODI) in the older adults [$R^2_{change} = 0.22$, $F_{change} = 12.26$, $P_{Fchange} = 0.001$, unstandardized beta = 0.000, 95% CI (0.000-0.000), SE = 0.000, standardized beta = -0.47 , $t = -3.50$, $P = 0.001$, Cohen's $F^2 = .28$]. No such associations were observed for either leisure activities or education (both $t < 0.05$, $P > 0.95$).

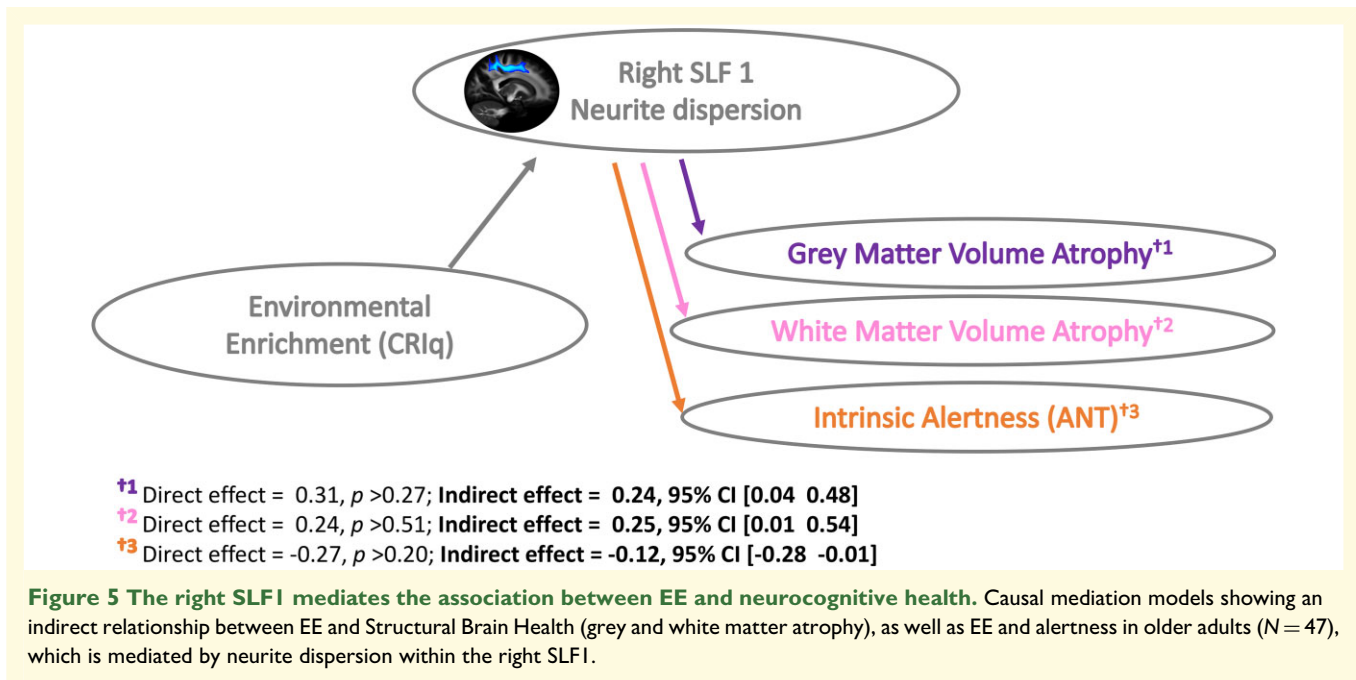
Follow-up analyses comparing model fits using the Bayesian inference criterion indicated that the best-fitting model for ODI of the right SLF1 contained the work subscale of the CRIq ($P(M|data) = 0.43$). More specifically, after observing the data, the odds of including CRIq work in a model of ODI of the right SLF1 increased by a factor of 14.44 ($BF_M = 14.44$). These odds were over five times the two next best-fitting models, which included a combination of work with education [Model 2: $P(M|data) = 0.09$; $BF_M = 2.7$] and work with leisure engagements [Model 3: $P(M|data) = 0.09$; $BF_M = 2.7$]. Model 4 contained a combination of all variables [i.e. work, education, leisure and age; $P(M|data) = 0.08$; $BF_M = 0.35$]. All other models had a posterior

probability ≤ 0.05 . This pattern of results suggests that in this cohort work is, by far, the strongest predictor of ODI in the right SLF1.

The right SLF1 mediates the association between EE and Structural Brain Health (grey and white matter atrophy)

To test whether ODI of the SLF relates to the structural health of the ageing brain, both grey matter and white volume (both normalized by head size) were modelled separately as a function of age and the six SLF tracts (SLF 1-3, left and right hemisphere). For grey matter volume atrophy (GMVa) when age was entered in the first step of the model, it offered no significant improvement in model fit over the intercept only model [$R^2_{change} = 0.01$, $F_{change} = 0.47$, $P_{Fchange} = 0.5$, unstandardized beta = -0.91 , 95% CI (-3.60 to 1.78), standardized beta = -0.10 ; SE = 1.33, $t = -0.68$, $P = 0.50$]. Next, ODI estimates for each of the six SLF branches were entered into the model of GM volume using a stepwise approach. This model offered a significant improvement in fit ($R^2_{change} = 0.17$, $F_{change} = 8.85$, $P_{Fchange} = 0.005$) and led to the inclusion of the right SLF1 [unstandardized beta = -1368.67 , 95% CI (-2296.17 to -441.57), standardized beta = -0.41 ; SE = 459.87, $t = -2.98$, $P = 0.005$, Cohen's $F^2 = 0.22$], and exclusion of all other SLF branches (all $t < 0.55$, $P > 0.58$), indicating that less dispersion of neurites (i.e. lower ODI) within the right SLF1 was associated with less GMVa (i.e. greater total GM volume). To obtain accurate parameter estimates of this model, not influenced by other uninformative variables, we modelled GMVa directly as a function of the right SLF1 and report the results in Table 3.

For WMVa, again age was entered as the first step in the model and offered no significant improvement in model fit [$R^2_{change} = 0.01$, $F_{change} = 0.34$, $P_{Fchange} = 0.56$, unstandardized beta = -0.95 , 95% CI (-4.26 to 2.35), standardized beta = -0.09 , SE = 1.64, $t = -0.58$, $P = 0.56$]. Adding the ODI estimates for the six SLF branches using a stepwise approach offered a significant improvement in fit ($R^2_{change} = 0.12$, $F_{change} = 5.99$, $P_{Fchange} = 0.02$) and again led to the inclusion of the right SLF1 [unstandardized beta = -1425.22 , 95% CI (-2598.94 to -251.5), standardized beta = -0.35 ; SE = 582.39, $t = -2.45$, $P = 0.02$, Cohen's $F^2 = 0.15$] and exclusion of all other SLF branches (all $t < 0.45$, $P > 0.41$), indicating that less dispersion of neurites (lower ODI) of the



right SLF1 was associated with less WMVa (i.e. larger total WM volume). To obtain accurate parameter estimates of this model, not influenced by other uninformative variables, we modelled WMVa directly as a function of the right SLF1 and report the results in Table 3.

To bolster these results, we employed Bayes Factor analyses. When modelling GMVa as a function of ODI for all six SLF branches and age, the best-fitting model was ODI of the right SLF1 [$P(M|data) = 0.43$; $BF_m = 41.26$], indicating that after observing the data, the odds of including neurite dispersion of the right SLF1 in a model for GMVa increased by a factor of 41.26. All other models had a posterior probability of < 0.05 . When the same analysis was repeated with WMVa, the best-fitting model was again ODI of the right SLF1 [$P(M|data) = 0.21$, $BF_m = 7.75$], indicating the odds of including right SLF1 ODI in a model for WMVa increased by a factor of 7.75. All other models had a posterior probability of < 0.05 .

Our results so far indicate that EE is associated with less neurite dispersion (ODI) of the right SLF1 and that less ODI within this specific tract is associated with less atrophy in both GM and WM. This raises the possibility that a causal relationship may exist such that the extent to which EE positively impacts structural brain health (i.e. offsets white and GMVa) is dependent, at least partly, on the degree to which EE has altered WM properties of the right SLF1. To formally test this hypothesis, we ran two causal mediation models ($EE \rightarrow ODI \text{ rSLF1} \rightarrow GMVa$; $EE \rightarrow ODI \text{ rSLF1} \rightarrow WMVa$). Bootstrapped mediation analyses showed an indirect effect for both GMVa [direct effect = 0.31, $P = 0.28$; indirect effect = 0.23, 95% CI (0.04–0.48)] and WMVa [direct effect = 0.24, $P = 0.51$; indirect effect = 0.25, 95% CI (0.01–0.54)]. This indicates that the degree to which EE positively mitigates GM and WM atrophy of the ageing brain is

dependent in part, on the degree to which EE has altered neurite dispersion properties of the right SLF1 (Fig. 5).

Neurite dispersion in the right SLF1 is associated with an alertness score

The results thus far demonstrate that EE facilitates superior maintenance of neurite (axonal) dispersion in older adults within the right SLF1. This suggests that the plasticity of the right SLF1 might be specifically sensitive to the beneficial effects of environmental enrichment on ageing brain health. To assess whether the right SLF1 showed a meaningful relationship to alertness, here we modelled this tract as a function of the three subscales of the ANT; alertness, orienting, conflict, see Fig. 4C). Age was entered as the first step in the model and offered no improvement on the intercept only model [$R^2_{\text{change}} = 0$, $F_{\text{change}} = 0.02$, $P_{F_{\text{change}}} = 0.88$, unstandardized beta = 0, 95% CI (-0.001 to 0.001), standardized beta = -0.02, SE = 0, $t = -0.16$, $P = 0.88$]. Next, we modelled the right SLF1 as a function of the three ANT subscales using a stepwise approach. This led to a significant improvement in model fit ($R^2_{\text{change}} = 0.09$, $F_{\text{change}} = 4.59$, $P_{F_{\text{change}}} = 0.04$) with neurite dispersion of the right SLF1 uniquely associated with the alertness [unstandardized beta = 0.000, 95% CI (0.000–0.000), SE = 0, standardized beta = 0.31, $t = 2.14$, $P = 0.04$, Cohen's $F^2 = 0.11$] but not orienting ($t = -1.00$, $P = 0.32$) or conflict ($t = -1.63$, $P = 0.11$) components of the task. To obtain accurate parameter estimates for the relationship between neurite dispersion of the right SLF1 and ANT alertness, we modelled the direct association without other uninformative signals and report the results in Table 3.

Follow-up Bayesian factor analyses revealed two models with a posterior probability of > 0.05 after having observed

the data. Of these, the best-fitting model included only the alertness score of the ANT [$P(M|data) = 0.19$], such that the odds of including ANT alertness in the model of the SLF1 were more than 4.5 times as high after observing the data ($BF_m = 4.51$). In contrast, both the posterior probability and the odds of the next best model were lower (model including the alertness and executive control subscales; $P(M|data) = 0.08$, $BF_m = 2.41$).

The right SLF1 mediates the association between EE and alertness

The findings thus far suggest that a lifetime of EE is associated with reduced neurite (axonal) dispersion within the right SLF1 in older adults. In addition, we observed that reduced right SLF1 neurite dispersion is consequential to cognition, such that it facilitates better maintenance of internal alertness in advanced age (Fig. 4). This raises the possibility of a causal association between these factors such that EE facilitates alertness by impacting the plasticity of the right SLF1. To test this hypothesis, we ran a causal mediation model; $EE \rightarrow ODI \rightarrow rSLF1 \rightarrow Alertness$ (Fig. 5). Bootstrapped mediation analyses (5000 samples) revealed a significant mediation such that EE was associated with superior WM microstructure (reduced neurite dispersion) within the right SLF1 which, in turn, facilitated better internal alertness. We note there was no direct relationship between EE and alertness, suggesting that the association between these two variables is dependent on WM properties of the right SLF1 [direct effect = -0.27 , $P = 0.21$; indirect effect = -0.1172 , 95% CI (-0.2837 to -0.0098)]. In accordance with the findings above which highlighted a privileged association between occupational engagements and ODI of the right SLF1, repeating the mediation model with the work subscale (as opposed to the composite CRIq score) additionally resulted in a significant mediation effect (direct effect = -0.1924 , $P = 0.44$; indirect effect = -0.1777 , 95% CI (-0.4018 to -0.0185)).

Discussion

In the present study, we examined how microstructural properties of the SLF varied according to exposure to EEs to subsequently influence markers of neurocognitive health in older adults. Our findings indicate that greater exposure to EEs across a lifetime is associated with reduced axonal dispersion within the right SLF1 in older adults. This in turn mitigates declines in structural brain health (assessed via GMVa and WMVa) and intrinsic alertness (captured with the well-validated ANT test). To the best of our knowledge, this is the first study providing direct evidence linking microstructural properties of a long-range association pathway within the right fronto-parietal networks (the right SLF1) to behavioural markers of neurocognitive reserve and brain health. Here we discuss how these results corroborate our previous work^{34–36} and that of others,³⁷ to provide further

experimental evidence in support of the hypothesis that EEs strengthen right hemisphere fronto-parietal networks to facilitate the phenomenon of cognitive reserve.^{19,20}

The findings presented here indicate that microstructure of the right SLF1 might be specifically sensitive to the beneficial effects of environmental enrichment on neurocognitive health in older adults. Brain matter volume, indicative of age-related atrophy, is often used as a proxy of ageing brain health.^{6,9,31–33} Previous theoretical and experimental work suggests that lifelong exposure to cognitive and social enrichment, providing the so-called cognitive reserve, can promote healthy cognitive function despite objective markers of vulnerability in the brain including atrophy³³ or disease-related neuropathological changes (e.g. Alzheimer's)⁵. Yet the mechanisms by which this reserve is facilitated have remained unclear.^{6,7,97} Here we observed that the extent to which neurite (axonal) dispersion is preserved within the right SLF1 is directly associated with both structural brain health (GMVa and WMVa) and cognitive function (intrinsic alertness on the ANT) in later years. More specifically, causal mediation models indicated that the associations between EE with both structural brain health and alertness were dependent on neurite dispersion of the right SLF1. This suggests that the benefits of EE to neurocognitive health in older adults depend, at least in part on the degree to which WM microstructural architecture within the right SLF1 has been altered. Future work should explore whether the beneficial effects of EE are specific to the right SLF (right fronto-parietal networks) or whether other networks also mediate the neurocognitive benefits of EE. It will be additionally important to identify whether the right SLF interacts with other structural markers of brain health including those particularly sensitive to age-related cognitive deficits (e.g. hippocampal atrophy).

Novel and complex environments require high levels of alertness, which in turn optimize the processing of upcoming signals.⁶⁷ Functionally linked with noradrenaline,^{98,99} alertness has been associated with right lateralized fronto-parietal networks and thalamic structures,^{16,66,73,100–103} with deficits in maintaining alertness reported following right but not left hemispheric strokes.⁷⁴ Given the hypothesized relevance of noradrenaline to neurocognitive resilience^{19,20} alertness is an ideal candidate to facilitate the beneficial consequences of EE. Our results presented here suggest that repeated exposure to EE, which likely necessitates high levels of alertness, reduces axonal dispersion within right hemisphere fronto-parietal networks, to exert beneficial effects on cognitive symptoms of ageing. Although causality cannot be inferred from our cross-sectional design, it is possible that a self-perpetuating relationship between the high levels of alertness required by EEs, well-established structural networks which support the cognitive capacity of alertness (right SLF1) and intrinsic alertness capacities. This would not only be directly in line with the hypothesis that alertness, through its association with the right lateralized noradrenergic system and the right fronto-parietal networks, is a critical determinant of cognitive reserve²⁰ but would also support

the rationale for designing interventions to maximally modulate alertness, through modulation of the noradrenergic system, in older adults. Given the foundational role of alertness in more global aspects of attention,¹⁰⁴ improving this facet of cognition may result in a cascade of benefits for the preservation of neurocognitive health in later years. Future longitudinal and intervention work should disentangle the causal directionality of these effects, underpinning the association between EE and microstructural WM changes within the SLF. This could be combined with pharmacological manipulations, non-invasive proxies of noradrenaline (e.g. pupillometry), and parallel work in animal models to assess whether the degree to which WM fronto-parietal plasticity is induced depends on noradrenergic action. Finally, it would be important to explore whether pre-existing individual differences in alertness and/or WM structure of the SLF influence the extent to which enrichment impacts the WM (i.e. the ‘chicken or egg’ question of cognitive reserve).

The SLF is a WM fronto-parietal association pathway that consists of three branches.³⁸ The most dorsal branch (the SLF1) has projections to the frontal eye fields, premotor cortex and the intraparietal sulcus¹⁸. These regions comprise a functional network often referred to as the dorsal attention or dorsal fronto-parietal network.^{100,105–107} This network is activated by internal goals and expectations and links the processing of sensory information, including the formation of perceptual decisions with relevant motor commands.^{42,106} As such, it is likely that WM architecture within the dorsal SLF facilitates the coordination and communication of information between sensory, decision and motor regions to subsequently influence the efficiency of an individual’s response.⁴² Our findings may suggest that a lifetime of intrinsic alertness ‘training’, afforded by high EE, may induce WM plasticity within the right SLF1 to facilitate better intrinsic alertness in older years. In our cohort, these effects were driven by the complexity of professional and occupational engagements. Future work in the larger population-level cohort and longitudinal ‘big data’ studies should investigate the optimal ways to induce WM plasticity within the right SLF1. In addition, future work should assess whether in vulnerable cohorts novel intervention techniques (e.g. brain stimulation and neurofeedback) could be used to induce similar changes to the structural organization within this pathway. Addressing these hypotheses would provide increasing support for the utility of the right SLF as a marker of resilience in older adults and facilitate translational avenues to optimize interventions aimed at preventing age-related cognitive decline.

The results presented in this manuscript raise the intriguing possibility that WM plasticity within the right fronto-parietal networks may be induced by EEs to facilitate resilience to cognitive decline later in life. Here we show that EE was associated with decreased dispersion of axons (lower ODI) specifically within the right SLF. Previous studies contrasting younger and older participants have indicated that increased dispersion of axons is one of the indicators of age-related brain changes indicative of poorer cognitive function.^{55,57,58,108} Moreover, previous reports assessing the

effect of age on WM have demonstrated that NODDI-derived measures outperform measures derived from DTI.⁵⁵ In agreement with Kodiveera *et al.*, our data similarly point to greater sensitivity of ODI compared with DTI-derived FA, such that our associations between the SLF and behaviour were observed specifically for ODI and not FA (although we found weak bayesian support for an association between FA of the right SLF2 with EE). Our findings are in line with growing evidence from both rodent and human studies that experience and training induce WM plasticity, reflected through changes in WM microstructural properties in the adult brain.^{29,109,110} One of the proposed mechanisms underlying this WM plasticity is activity-dependent changes in myelination (for review see Sampaio-Baptista *et al.*¹¹¹). Myelination and the NODDI-derived parameters used here are somewhat related but predominantly complementary measures of WM microstructure.^{57,112} Thus, future investigations with both animal and human participants should disentangle the precise biological basis underpinning the impact of a lifetime of EE on neurocognitive health. As one of the limitations of the present study is cross-sectional design, any future work should also aim to gather evidence from longitudinal studies directly exploring any relationships. It should be also noted here that despite improved estimations of microstructural features of the WM with NODDI compared with DTI, ODI (axonal dispersion) measures, which estimate the degree of fibre coherence, could be still affected by crossing with other WM tracts. As such, it is possible that our findings could be driven, at least to some extent by changes to other right fronto-parietal pathways which cross the SLF1.

One caveat to our findings is that factors which may have drawn individuals to high levels of EE throughout their lifetime (including socio-economic demographics, personality, genetic and early-life cognitive abilities) were not available for investigation. As such we cannot rule out the possibility that alternative mediating factors are contributing to our observed associations between environment, the brain, and behaviour. However, several points suggest this was not the case. First, previous work with monozygotic (identical) twin studies has shown EE positively impacts cognition over and above genetic factors.¹¹³ Moreover, our effects of EE were driven by the professional and not education subscale of the CRIq, suggesting that early-life cognitive engagement was not the critical influence in this cohort. Finally, increasing evidence suggests that the ageing brain maintains sufficient plasticity such that it can be targeted in later years to increase reserve and resilience.^{114–116} Thus, further work providing insights into multiple factors accounting for the diverse cognitive ageing trajectories and examining the complex interplay between the different facets of EE throughout the lifespan is required to design the best possible and perhaps personalized interventions mitigating or preventing age-related cognitive decline.

Estimating exposure to EEs is challenging for several reasons. For example, it is possible that on an individual level, different factors (proxy measures, or the degree of *engagement* with, as opposed to *exposure* to, a given environment)¹¹⁷ will impact the extent to which EE positively

benefits neurocognitive health. In other words, perhaps the type of environmental enrichment is less important than the level of cognitive engagement and alertness demanded which determines the extent to which the right hemisphere SLF is strengthened. In addition, different proxy measures have different lifetime dimensions and timescales of impact e.g. childhood versus early adulthood versus later years.¹¹⁸ We propose that the complex issue of how best to increase brain resilience is best addressed through large longitudinal studies incorporating big data, activity tracking and experiential sampling. Here, we provide an objective marker in the brain that can be trialled in these larger trials as a candidate pathway supporting cognitive resilience in later years.

Although the beneficial effects of EE for neurocognitive resilience are well established, the mechanisms by which this occurs are still under considerable debate. The findings presented here, in concert with our previous findings,^{34,36} suggest that anatomical properties within the right fronto-parietal networks might be neural correlates of resilience in the ageing brain. In further support of this hypothesis, brain stimulation targeting the right fronto-parietal networks not only improves behavioural and EEG markers of attention but also temporarily alters the lateralized impact of lifetime experiences in low reserve individuals such that it resembles that of their high reserve peers.^{34,35} Although neuropathological markers of Alzheimer's disease are associated with cognitive deficits, over 50% of the variability in symptomatology still remains unexplained.^{119,120} We propose that WM properties of the right FPN be tested as objective markers of resilient neurocognitive ageing to help capture the heterogeneity associated with the clinical presentation of Alzheimer's disease and be used to assay the efficacy of interventions aimed at ameliorating age-related cognitive decline.

Acknowledgements

We warmly thank the volunteers from the School of Psychology panel and the Birmingham 1000 Elders group for participation in this study.

Funding

This work was supported by the Birmingham-Nottingham Strategic Collaboration Fund (BNSCF336 to S.N.S. and M.C.) and by a Wellcome Trust Institutional Strategic Support Fund critical data award (204846/Z/16/Z to M.C.). M.C. was supported with a Birmingham-Illinois Partnership for Discovery, Engagement and Education (BRIDGE) Fellowship, M.B.B. was supported with a Marie Skłodowska-Curie Fellowship from the European Commission (AGEING PLASTICITY; grant number 844246), and S.N.S. was supported by the Wellcome Trust (217266/Z/19/Z) and by an European Research Council Consolidator Grant (101000969). This work was additionally supported by the National Institute for Health

Research (NIHR) Oxford Health Biomedical Research Centre and the Wellcome Centre for Integrative Neuroimaging was supported by core funding from the Wellcome Trust (203139/Z/16/Z).

Ethics

The study was approved by the University of Birmingham Ethical Review Committee. All participants provided written informed consent in agreement with the approved ethics protocol (ERN_110429AP66).

Competing interests

The authors declare no competing interests.

Supplementary material

Supplementary material is available at *Brain Communications* online.

References

- Livingston G, Huntley J, Sommerlad A, *et al.* The Lancet Commissions Dementia prevention, intervention, and care: 2020 report of the Lancet Commission. *Lancet*. 2020;396:413–446.
- Stern Y, Alexander GE, Prohovnik I, Mayeux R. Inverse relationship between education and parietotemporal perfusion deficit in Alzheimer's disease. *Ann Neurol*. 1992;32:371–375.
- Bennett DA, Schneider JA, Tang Y, Arnold SE, Wilson RS. The effect of social networks on the relation between Alzheimer's disease pathology and level of cognitive function in old people: A longitudinal cohort study. *Lancet Neurol*. 2006;5:406–412.
- Stern Y, Arenaza-Urquijo EM, Bartrés-Faz D, *et al.* Whitepaper: Defining and investigating cognitive reserve, brain reserve, and brain maintenance. *Alzheimers Dement*. 2020;16:1305–1311.
- Xu H, Yang R, Qi X, *et al.* Association of lifespan cognitive reserve indicator with dementia risk in the presence of brain pathologies. *JAMA Neurol*. 2019;76:1184–1191.
- Cabeza R, Albert M, Belleville S, *et al.* Maintenance, reserve and compensation: The cognitive neuroscience of healthy ageing. *Nat Rev Neurosci*. 2018;19:701–710.
- Stern Y, Chételat G, Habeck C, *et al.* Mechanisms underlying resilience in ageing. *Nat Rev Neurosci*. 2019;20(4):246.
- Cabeza R, Albert M, Belleville S, *et al.* Reply to 'Mechanisms underlying resilience in ageing'. *Nat Rev Neurosci*. 2019;20(4):247.
- Stern Y. Cognitive reserve in ageing and Alzheimer's disease. *Lancet Neurol*. 2012;11:1006–1012.
- Valenzuela M, Sachdev P. Brain reserve and dementia: A systematic review. *Psychol Med*. 2006;36:441–454.
- Opdebeeck C, Martyr A, Clare L. Cognitive reserve and cognitive function in healthy older people: A meta-analysis. *Ageing Neuropsychol Cogn*. 2016;23:40–60.
- Nelson ME, Jester DJ, Petkus AJ, Andel R. Cognitive reserve, Alzheimer's neuropathology, and risk of dementia: A systematic review and meta-analysis. *Neuropsychol Rev*. 2021;31:233–250.
- Beck DM, Rees G, Frith CD, Lavie N. Neural correlates of change detection and change blindness. *Nat Neurosci*. 2001;4(6):645–650.

14. Naghavi HR, Nyberg L. Common fronto-parietal activity in attention, memory, and consciousness: Shared demands on integration? *Conscious Cogn.* 2005;14:390–425.
15. Hester R, Foxe JJ, Mollholm S, Shpaner M, Garavan HP. Neural mechanisms involved in error processing: A comparison of errors made with and without awareness. *Neuroimage.* 2005;27:602–608.
16. Singh-Curry V, Husain M. The functional role of the inferior parietal lobe in the dorsal and ventral stream dichotomy. *Neuropsychologia.* 2009;47:1434–1448.
17. Stuss DT. Functions of the frontal lobes: Relation to executive functions. *J Int Neuropsychol Soc.* 2011;17:759–765.
18. Stuss DT, Knight RT. *Principles of frontal lobe function.* 2nd edn. Oxford University Press; 2013.
19. Robertson IH. A noradrenergic theory of cognitive reserve: Implications for Alzheimer's disease. *Neurobiol Aging.* 2013;34:298–308.
20. Robertson IH. A right hemisphere role in cognitive reserve. *Neurobiol Aging.* 2014;35:1375–1385.
21. Oke A, Keller R, Mefford I, Adams RN. Lateralization of norepinephrine in human thalamus. *Science.* 1978;200:1411–1413.
22. Robinson RG. Differential behavioral and biochemical effects of right and left hemispheric cerebral infarction in the rat. *Science.* 1979;205:707–710.
23. Grefkes C, Wang LE, Eickhoff SB, Fink GR. Noradrenergic modulation of cortical networks engaged in visuomotor processing. *Cereb Cortex.* 2010;20:783–797.
24. Jodo E, Aston-Jones G. Activation of locus coeruleus by prefrontal cortex is mediated by excitatory amino acid inputs. *Brain Res.* 1997;768:327–332.
25. Jodoj E, Chiang C, Aston-Jones G. Potent excitatory influence of prefrontal cortex activity on noradrenergic locus coeruleus neurons. *Neuroscience.* 1998;83:63–79.
26. Singewald N, Philippu A. Release of neurotransmitters in the locus coeruleus. *Prog Neurobiol.* 1998;56:237–267.
27. Shalev N, Vangkilde S, Neville MJ, Tunbridge EM, Nobre AC, Chechlacz M. Dissociable catecholaminergic modulation of visual attention: Differential effects of catechol-o-methyltransferase and dopamine beta-hydroxylase genes on visual attention. *Neuroscience.* 2019;412:175–189.
28. Draganski B, Gaser C, Busch V, Schuierer G, Bogdahn U, May A. Changes in grey matter induced by training. *Nature.* 2004;427:311–312.
29. Scholz J, Klein MC, Behrens TEJ, Johansen-Berg H. Training induces changes in white-matter architecture. *Nat Neurosci.* 2009;12:1370–1371.
30. Woollett K, Maguire EA. Acquiring 'the Knowledge' of London's layout drives structural brain changes. *Curr Biol.* 2011;21:2109–2114.
31. Lövdén M, Bodammer N, Kühn S, et al. Experience-dependent plasticity of white-matter microstructure extends into old age. *Neuropsychologia.* 2010;48:3878–3883.
32. Barulli D, Stern Y. Efficiency, capacity, compensation, maintenance, plasticity: Emerging concepts in cognitive reserve. *Trends Cogn Sci.* 2013;17:502–509.
33. Chan D, Shafto M, Kievit R, et al. Lifestyle activities in mid-life contribute to cognitive reserve in late-life, independent of education, occupation, and late-life activities. *Neurobiol Aging.* 2018;70:180–183.
34. Brosnan MB, Demaria G, Petersen A, Dockree PM, Robertson IH, Wiegand I. Plasticity of the right-lateralized cognitive reserve network in ageing. *Cereb Cortex.* 2017;28:1749–1759.
35. Brosnan MB, Arvaneh M, Harty S, et al. Prefrontal modulation of visual processing and sustained attention in aging, a transcranial direct current stimulation–electroencephalogram coregistration approach. *J Cogn Neurosci.* 2018;30:1630–1645.
36. Shalev N, Brosnan MB, Chechlacz M. Right lateralized brain reserve offsets age-related deficits in ignoring distraction. *Cereb Cortex Commun.* 2020;1:1–13.
37. Van Loenhoud AC, Wink AM, Groot C, et al. A neuroimaging approach to capture cognitive reserve: Application to Alzheimer's disease. *Hum Brain Mapp.* 2017;38:4703–4715.
38. de Schotten M T, Dell'Acqua F, Forkel SJ, et al. A lateralized brain network for visuospatial attention. *Nat Neurosci.* 2011;14:1245–1246.
39. Chechlacz M, Humphreys GW, Sotiropoulos SN, Kennard C, Cazzoli D. Structural organization of the corpus callosum predicts attentional shifts after continuous theta burst stimulation. *J Neurosci.* 2015;35:15353–15368.
40. Marshall TR, Bergmann TO, Jensen O. Frontoparietal structural connectivity mediates the top-down control of neuronal synchronization associated with selective attention. *PLoS Biol.* 2015;13(10):e1002272.
41. Deligianni F, Carmichael DW, Zhang GH, Clark CA, Clayden JD. NODDI and tensor-based microstructural indices as predictors of functional connectivity. *PLoS One.* 2016;11:e0153404.
42. Brosnan MB, Sabarodin K, Silk T, et al. Evidence accumulation during perceptual decisions in humans varies as a function of dorsal frontoparietal organization. *Nat Hum Behav.* 2020;4:844–855.
43. Chechlacz M, Gillebert CR, Vangkilde SA, Petersen A, Humphreys GW. Structural variability within frontoparietal networks and individual differences in attentional functions: An approach using the theory of visual attention. *J Neurosci.* 2015;35:10647–10658.
44. Raz N, Rodrigue KM. Differential aging of the brain: Patterns, cognitive correlates and modifiers. *Neurosci Biobehav Rev.* 2006;30:730–748.
45. Barrick TR, Charlton RA, Clark CA, Markus HS. White matter structural decline in normal ageing: A prospective longitudinal study using tract-based spatial statistics. *Neuroimage.* 2010;51:565–577.
46. Burzynska AZ, Preuschhof C, Bäckman L, et al. Age-related differences in white matter microstructure: Region-specific patterns of diffusivity. *Neuroimage.* 2010;49:2104–2112.
47. Westlye LT, Walhovd KB, Dale AM, et al. Life-span changes of the human brain white matter: Diffusion tensor imaging (DTI) and volumetry. *Cereb Cortex.* 2010;20:2055–2068.
48. Lerch JP, van der Kouwe AJW, Raznahan A, et al. Studying neuroanatomy using MRI. *Nat Neurosci.* 2017;20(20):314–326.
49. Assaf Y, Basser PJ. Composite hindered and restricted model of diffusion (CHARMED) MR imaging of the human brain. *Neuroimage.* 2005;27:48–58.
50. Zhang H, Schneider T, Wheeler-Kingshott CA, Alexander DC. NODDI: Practical in vivo neurite orientation dispersion and density imaging of the human brain. *Neuroimage.* 2012;61:1000–1016.
51. Alexander D, Dyrby T, Nilsson M, Zhang H. Imaging brain microstructure with diffusion MRI: Practicality and applications. *NMR Biomed.* 2019;32:e3841.
52. Sexton C, Walhovd K, Storsve A, et al. Accelerated changes in white matter microstructure during aging: A longitudinal diffusion tensor imaging study. *J Neurosci.* 2014;34:15425–15436.
53. Pierpaoli C, Basser PJ. Toward a quantitative assessment of diffusion anisotropy. *Magn Reson Med.* 1996;36:893–906.
54. Beaulieu C. The biological basis of diffusion anisotropy. In: *Diffusion MRI from quantitative measurement to in vivo neuroanatomy.* 2nd edn. Academic Press; 2014:155–183.
55. Kodiweera C, Alexander A, Harezlak J, McAllister T, Wu Y. Age effects and sex differences in human brain white matter of young to middle-aged adults: A DTI, NODDI, and q-space study. *Neuroimage.* 2016;128:180–192.
56. Kunz N, Zhang H, Vasung L, et al. Assessing white matter microstructure of the newborn with multi-shell diffusion MRI and biophysical compartment models. *Neuroimage.* 2014;96:288–299.
57. Billiet T, Vandenbulcke M, Mädler B, et al. Age-related microstructural differences quantified using myelin water imaging and advanced diffusion MRI. *Neurobiol Aging.* 2015;36:2107–2121.

58. Chang YS, Owen JP, Pojman NJ, *et al.* White matter changes of neurite density and fiber orientation dispersion during human brain maturation. *PLoS One*. 2015;10:e0123656.
59. Adluru G, Gur Y, Anderson JS, *et al.* Assessment of white matter microstructure in stroke patients using NODDI. *Annu Int Conf IEEE Eng Med Biol Soc IEEE Eng Med Biol Soc Annu Int Conf*. 2014;2014:742–745.
60. Billiet T, Mädler B, D'Arco F, *et al.* Characterizing the microstructural basis of 'unidentified bright objects' in neurofibromatosis type 1: A combined in vivo multicomponent T2 relaxation and multi-shell diffusion MRI analysis. *Neuroimage (Amst)*. 2014;4: 649–658.
61. Winston GP, Micallef C, Symms MR, Alexander DC, Duncan JS, Zhang H. Advanced diffusion imaging sequences could aid assessing patients with focal cortical dysplasia and epilepsy. *Epilepsy Res*. 2014;108:336–339.
62. Timmers I, Zhang H, Bastiani M, Jansma BM, Roebroek A, Rubio-Gozalbo ME. White matter microstructure pathology in classic galactosemia revealed by neurite orientation dispersion and density imaging. *J Inherit Metab Dis*. 2015;38:295–304.
63. Veldsman M, Tai XY, Nichols T, *et al.* Cerebrovascular risk factors impact frontoparietal network integrity and executive function in healthy ageing. *Nat Commun*. 2020;11:1–10.
64. Merluzzi AP, Dean DC III, Adluru N, *et al.* Age-dependent differences in brain tissue microstructure assessed with neurite orientation dispersion and density imaging. *Neurobiol Aging*. 2016;43:79.
65. Fan J, McCandliss B, Sommer T, Raz A, P MI. Testing the efficiency and independence of attentional networks. *J Cogn Neurosci*. 2002;14:340–347.
66. Fan J, McCandliss B, Fossella J, Flombaum J, Posner MI. The activation of attentional networks. *Neuroimage*. 2005;26:471–479.
67. Petersen SE, Posner MI. The attention system of the human brain: 20 years after. *Annu Rev Neurosci*. 2012;35:73–89.
68. Nucci M, Mapelli D, Mondini S. Cognitive Reserve Index questionnaire (CRIq): A new instrument for measuring cognitive reserve. *Aging Clin Exp Res*. 2012;24:218–226.
69. Fernandez-Duque D, Black S. Attentional networks in normal aging and Alzheimer's disease. *Neuropsychology*. 2006;20: 133–143.
70. Jennings J, Dagenbach D, Engle C, Funke L. Age-related changes and the attention network task: An examination of alerting, orienting, and executive function. *Neuropsychol Dev Cogn B Aging Neuropsychol Cogn*. 2007;14:353–369.
71. Ishigami Y, Klein RM. Repeated measurement of the components of attention of older adults using the two versions of the attention network test: Stability, isolability, robustness, and reliability. *Front Aging Neurosci*. 2011;3:17.
72. Mcdonough IM, Wood MM, Miller WS. A review on the trajectory of attentional mechanisms in aging and the Alzheimer's disease continuum through the attention network test. *Yale J Biol Med*. 2019;92:37–51.
73. Posner MI, Petersen SE. The attention system of the human brain. *Annu Rev Neurosci*. 1990;13:25–42.
74. Posner MI. Measuring alertness. *Ann N Y Acad Sci*. 2008;1129: 193–199.
75. Andersson JL, Skare S, Ashburner J. How to correct susceptibility distortions in spin-echo echo-planar images: Application to diffusion tensor imaging. *Neuroimage*. 2003;20(2):870–888.
76. Alfaro-Almagro F, Jenkinson M, Bangerter NK, *et al.* Image processing and Quality Control for the first 10,000 brain imaging datasets from UK Biobank. *Neuroimage*. 2018;166:400–424.
77. Andersson JL, Jenkinson M, Smith S. Non-linear registration Aka spatial normalisation. Internal Technical Report TR07JA2. Oxford Centre for Functional Magnetic Resonance Imaging of the Brain, Department of Clinical Neurology, OxfordUniversity, 2007. www.fmrib.ox.ac.uk/analysis/techrep.
78. Andersson JL, Smith S, Jenkinson M. Non-linear optimisation. Internal Technical Report TR07JA1. Oxford Centre for Functional Magnetic Resonance Imaging of the Brain, Department of Clinical Neurology, Oxford University, 2007. www.fmrib.ox.ac.uk/analysis/techrep.
79. Zhang Y, Brady M, Smith S. Segmentation of brain MR images through a hidden Markov random field model and the expectation-maximization algorithm. *IEEE Trans Med Imaging* 2001;20:45–57.
80. Smith SM, Zhang Y, Jenkinson M, *et al.* Accurate, robust, and automated longitudinal and cross-sectional brain change analysis. *Neuroimage* 2002;17:479–489.
81. Andersson JLR, Sotiropoulos SN. An integrated approach to correction for off-resonance effects and subject movement in diffusion MR imaging. *Neuroimage* 2016;125:1063–1078.
82. Jenkinson M, Smith S. A global optimisation method for robust affine registration of brain images. *Med Image Anal* 2001;5(2): 143–156.
83. Jenkinson M, Bannister P, Brady J, Smith S. Improved optimisation for the robust and accurate linear registration and motion correction of brain images. *NeuroImage* 2002;17(2):825–841.
84. Tariq M, Schneider T, Alexander D, Gandini Wheeler-Kingshott C, Zhang H. Bingham-NODDI: Mapping anisotropic orientation dispersion of neurites using diffusion MRI. *Neuroimage* 2016; 133:207–223.
85. Hernandez-Fernandez M, Reguly I, Jbabdi S, Giles M, Smith S, Sotiropoulos SN. Using GPUs to accelerate computational diffusion MRI: From microstructure estimation to tractography and connectomes. *Neuroimage* 2019;188:598–615.
86. Basser PJ, Mattiello J, Lebihan D. Estimation of the effective self-diffusion tensor from the NMR spin echo. *J Magn Reson Ser B* 1994;103:247–254.
87. de Groot M, Vernooij M, Klein S, *et al.* Improving alignment in Tract-based spatial statistics: Evaluation and optimization of image registration. *Neuroimage* 2013;76:400–411.
88. Warrington S, Bryant KL, Khrapitchev AA, *et al.* XTRACT - Standardised protocols for automated tractography in the human and macaque brain. *Neuroimage* 2020;217:116923.
89. Behrens TEJ, Berg HJ, Jbabdi S, Rushworth MFS, Woolrich MW. Probabilistic diffusion tractography with multiple fibre orientations: What can we gain? *Neuroimage* 2007;34:144–155.
90. Hayes AF. PROCESS: A versatile computational tool for observed variable mediation, moderation, and conditional process modeling. 2012.
91. Hayes AF. Introduction to mediation, moderation, and conditional process analysis: A regression-based approach. 2013.
92. Dienes Z. How Bayes factors change scientific practice. *J Math Psychol*. 2016;72:78–89.
93. Wagenmakers EJ, Love J, Marsman M, Jamil T, Ly A, Verhagen J, *et al.* Bayesian inference for psychology. Part II: Example applications with JASP. *Psychon Bull Rev*. 2018;25:58–76.
94. Schwarz G. Estimating the dimension of a model. *Ann Stat*. 1978; 6:461–464.
95. Jeffreys H. Theory of probability. In *Oxford classic texts in the physical sciences*. 3rd edn. Oxford University Press; 1961.
96. Wetzels R, Matzke D, Lee MD, Rouder JN, Iverson GJ, Wagenmakers EJ. Statistical evidence in experimental psychology: An empirical comparison using 855 t tests. *Perspect Psychol Sci*. 2011;6(3):291–298.
97. Husain M. Speak, memory: On cognitive reserve and brain resilience. *Brain*. 2021;144:1927–1928.
98. Aston-Jones G, Cohen JD. An integrative theory of locus coeruleus-norepinephrine function: Adaptive gain and optimal performance. *Annu Rev Neurosci*. 2005;28:403–450.
99. Marrocco RT, Davidson MC. Neurochemistry of attention. In: Parasuraman R, ed. *The attentive brain*. The MIT Press; 1998:35–50.
100. Corbetta M, Shulman GL. Control of goal-directed and stimulus-driven attention in the brain. *Nat Rev Neurosci*. 2002;3:201–215.
101. Corbetta M, Shulman GL. Spatial neglect and attention networks. *Annu Rev Neurosci*. 2011;34:569–599.

102. Sturm W, Willmes K. On the functional neuroanatomy of intrinsic and phasic alertness. *Neuroimage*. 2001;14:S76–S84.
103. Coull JT, Nobre AC, Frith CD. The noradrenergic $\alpha 2$ agonist clonidine modulates behavioural and neuroanatomical correlates of human attentional orienting and alerting. *Cereb Cortex*. 2001; 11:73–84.
104. Raz A, Buhle J. Typologies of attentional networks. *Nat Rev Neurosci*. 2006;7(5):367–379.
105. Fox MD, Corbetta M, Snyder AZ, Vincent JL, Raichle ME. Spontaneous neuronal activity distinguishes human dorsal and ventral attention systems. *Proc Natl Acad Sci USA*. 2006;103: 10046–10051.
106. Corbetta M, Patel G, Shulman GL. The reorienting system of the human brain: From environment to theory of mind. *Neuron*. 2008;58:306–324.
107. Vincent JL, Kahn I, Snyder AZ, Raichle ME, Buckner RL. Evidence for a frontoparietal control system revealed by intrinsic functional connectivity. *J Neurophysiol*. 2008;100:3328–3342.
108. Nazeri A, Chakravarty M, Rotenberg D, et al. Functional consequences of neurite orientation dispersion and density in humans across the adult lifespan. *J Neurosci*. 2015;35:1753–1762.
109. Blumenfeld-Katzir T, Pasternak O, Dagan M, Assaf Y. Diffusion MRI of structural brain plasticity induced by a learning and memory task. *PLoS One*. 2011;6:e20678.
110. Sampaio-Baptista C, Khrapitchev AA, Foxley S, et al. Motor skill learning induces changes in white matter microstructure and myelination. *J Neurosci*. 2013;33:19499–19503.
111. Sampaio-Baptista C, Johansen-Berg H. White matter plasticity in the adult brain. *Neuron*. 2017;96:1239–1251.
112. Fukutomi H, Glasser M, Zhang H, et al. Neurite imaging reveals microstructural variations in human cerebral cortical gray matter. *Neuroimage*. 2018;182:488–499.
113. Lee T, Lipnicki DM, Crawford JD, et al. Leisure activity, health, and medical correlates of neurocognitive performance among monozygotic twins: The older Australian twins study. *J Gerontol Ser B Psychol Sci Soc Sci*. 2013;69:514–522.
114. Edwards JD, Xu H, Clark DO, Guey LT, Ross LA, Unverzagt FW. Speed of processing training results in lower risk of dementia. *Alzheimers Dement Transl Res Clin Interv*. 2017;3:603–611.
115. Lenehan ME, Summers MJ, Saunders NL, et al. Sending your grandparents to university increases cognitive reserve: The tasmanian healthy brain project. *Neuropsychology*. 2016;30:525–531.
116. Peeters G, Kenny RA, Lawlor B. Late life education and cognitive function in older adults. *Int J Geriatr Psychiatry*. 2020;35: 633–639.
117. Park DC, Lodi-Smith J, Drew L, et al. The impact of sustained engagement on cognitive function in older adults: The synapse project. *Psychol Sci*. 2014;25(1):103–112.
118. Kartschmit N, Mikolajczyk R, Schubert T, Lacruz ME. Measuring cognitive rReserve (CR) - A systematic review of measurement properties of CR questionnaires for the adult population. *PLoS One*. 2019;14(8):e0219851.
119. Boyle PA, Yu L, Wilson RS, Leurgans SE, Schneider JA, Bennett DA. Person-specific contribution of neuropathologies to cognitive loss in old age. *Ann Neurol*. 2018;83:74–83.
120. Boyle PA, Wang T, Yu L, et al. To what degree is late life cognitive decline driven by age-related neuropathologies? *Brain*. 2021;144: 2166–2175.